

Design and evaluation of an instrumented floor tile for measuring older adults' cardiac function at home

Isaac Sung Jae Chang BASc^{a,*}

Abdul Qadir Javaid PhD^b

Jennifer Boger PhD^c

Amaya Arcelus PhD^d

Alex Mihailidis PhD^{a,b,d}

^aInstitute of Biomaterials and Biomedical Engineering (IBBME), University of Toronto, Toronto, ON, M5S 3G9, Canada; ^bDepartment of Occupational Science and Occupational Therapy, University of Toronto, Toronto, ON, M5S 3G9, Canada; ^cSystems Design Engineering, University of Waterloo, Waterloo, ON, N2L 3G1, Canada; ^dToronto Rehab Institute-UHN, Toronto, ON, M5G 2A2, Canada; *Corresponding author: isaac.chang@mail.utoronto.ca

I.S.J. Chang, A.Q. Javaid, J. Boger, A. Arcelus, A. Mihailidis. Design and evaluation of an instrumented floor tile for measuring older adults' cardiac function at home. Gerontechnology 2018;17(2):77-89; ; <https://doi.org/10.4017/gt.2018.17.2.002.00> **Background** Home monitoring of chronic diseases among older adults has been the focus of recent research as early detection of adverse events allows better management. Conventional medical devices require active engagement from the users, making it difficult to implement for people who have challenges with using technology, such as people with cognitive impairment. While smart homes are a promising emerging approach to tackle this challenge, related technologies are still cumbersome to use. In response to this challenge, we present a zero-effort instrumented floor tile that could be permanently installed in a bathroom or kitchen to measure a person's ballistocardiogram (BCG) and electrocardiogram (ECG) signals as part of a smart home system. **Methods** The floor tile contained four load cells in a Wheatstone bridge configuration to measure BCG while standing and four electrodes to measure ECG while sitting. Both the BCG and ECG were amplified by 100dB and had rails of -9V to +9V. BCG and ECG from the tile were sampled at 128Hz. To validate the device, data were collected from 60 healthy adults in various sitting and standing scenarios. The ECG and BCG obtained from the tile compared to RR-intervals (time duration between two successive ECG R-peaks) and heart rate obtained from chest ECG collected with (gold standard) gel-based electrodes. The RJ-interval (time duration between the ECG R-peak and the highest peak in the BCG signal called the J-peak) was also examined for an induced change in blood pressure. **Results** The ECG signal measured from the tile in the sitting position had 89% agreement with the gold standard ECG. Heart rate based on BCG had an error of $1.8 \pm 4.3\%$ compared to that of the gold standard ECG. The RJ-interval was reduced post-induced blood pressure change and returned to the baseline after a few seconds, which is comparable to the literature. **Conclusions** The prototype tile presented in this work shows promising results as a zero-effort component in a smart home vitals monitoring system. With further modification and addition of intelligent algorithms, we believe the tile presented could collect ECG and BCG from older adults in a non-clinical setting.

Keywords: Ballistocardiogram (BCG), electrocardiogram (ECG), ambient assisted living, zero-effort technology, cardiovascular monitoring

INTRODUCTION

Home monitoring of medical conditions has been a recent focus of research and development because of the potential benefit to older adults. In a recent report, 85% of Canadians between 65 and 79 years of age and 90% of

Canadians over 80 years of age have at least one chronic condition¹. Heart failure (HF), a prominent cardiovascular disease, is one such condition that benefits from regular monitoring of vital signs as this enables the disease to be managed as effectively as possible. HF is

a progressive disorder in which the heart fails to adequately supply blood to the body. In the United States, HF accounted for 36% of cardiovascular disease related deaths in 2016² and direct and indirect costs associated with HF are currently estimated to be \$30.7 billion annually³. One reason for the elevated costs is the high re-admission rate for HF after discharge as 24% of the patients are re-hospitalized due to worsening of the condition⁴.

One potential method to lower the mortality and re-admission rate is to continuously monitor patients at home so that the condition can be managed appropriately. To explore this method, multiple long-term studies have been conducted to evaluate the efficacy of home monitoring using the conventional medical equipment. While some studies showed that there is no difference between continuous monitoring and usual care⁵⁻⁷, other studies produced evidence that continuous monitoring resulted in a significant reduction in mortality rates, re-hospitalization rates and/or days in hospital⁷⁻⁹. While these results are encouraging, all these studies relied on conventional medical equipment and the ability and willingness of the participants to measure the vital signs regularly⁶. This requirement of active user engagement as well as issues such as non-compliance makes to monitoring method significantly difficult for a large portion of the population affected by HF, especially people with cognitive impairment. While most of the studies above excluded people with cognitive impairment, an estimated 28% of Medicare beneficiaries aged 65 and older had HF in addition to dementia in 2013, which approximately translates to more than 1 million people in the United States alone¹⁰. As such, usage of conventional medical equipment to monitor HF at home is not a viable option for people with HF and one or more co-morbidities that prevents the reliable use of home monitoring technologies.

Unobtrusive monitoring, in which monitoring parameters are collected via ambient sensors embedded in the home environment, is an emerging approach that has the potential to address these challenges. While the readiness level of the technology is still low (i.e., most are in the early prototyping stage)¹¹, more advanced monitoring devices continue to emerge, opening new and more reliable ways to apply the technology to improve unobtrusive health monitoring. Muse et al. give a perspective on the future of smart home where autonomous and unobtrusive monitoring devices perform medical assessment¹². The authors envision a smart home in which an older adult is awoken according to her optimum waking time determined by the bed based on her circadian rhythm and vital signs during sleep. Sensors on the hallway assess balance and gait as

she walks along the hallway to the bathroom. In the bathroom, the mirror and the floor tile check her weight, heart rate, blood pressure, and other parameters (e.g., cardiac output and pulse wave velocity). The mirror also reminds her of the medication that she should take on that day. As she sits on the toilet seat, the system comprised of the seat and the tile measures the weight and vital signs.

Our group shares the perspective presented by Muse et. al and is currently working towards the design of a smart home for measuring vitals and other metrics for supporting health. This paper presents our work into the creation of an instrumented floor tile (hereafter referred to as “smart floor tile” or “the tile”) that can measure heart rate during standing and sitting positions. In the design process, we adopted the design principle of ‘zero-effort technology’¹³, which is defined as the technology that requires little or no effort from the user for operation. In other words, the technology shifts the physical and mental burden of operation from the user to the technology itself¹³. The smart floor tile performs monitoring by collecting electrocardiogram (ECG) from the feet while sitting (sitting-F-ECG) and ballistocardiogram (BCG) while standing (standing-BCG), which is defined as a measure of reactive movement of the body in response to the flow of blood in the aorta and other vessels¹⁴.

ECG is chosen since it is particularly useful signal to retrieve temporal parameters such as HR, and heart rate variability (HRV), as well as any cardiac muscle abnormalities (e.g., myocardial ischemia). ECG however, is limited to monitoring the electrical activity of the heart; it cannot measure vascular measurements such as systolic time intervals and stroke volume. These parameters are related to the mechanical health of the heart, which is part of the standard assessment of cardiac function^{15,16}, and can be assessed by BCG.

In recent years, BCG has re-emerged as a signal that can provide mechanical information of the heart activity, in particular, parameters related to left ventricular function such as stroke volume or pre-ejection period (PEP)^{14,16,17}. BCG can be acquired from four different form factors: standing (i.e., longitudinal), sitting, lying down (i.e., transversal), and wearable¹⁶. Devices used to record BCG include modified weighing scales that collect standing-BCG^{17,18}, a chair that collects sitting-BCG¹⁹, a bed that collects transversal-BCG^{20,21}, and wearable devices on the ear or chest that collect wearable-BCG (chest vibrations)^{22,23}. All of the above mentioned devices are currently in the prototype phase with the exception of a commercialized weighing scale²⁴. Unlike the weighing scale, our floor tile collects standing-BCG without the user having to turn it on or do any initial-

An instrumented floor tile

sation and is intended for use by elderly adults in real-world contexts as part of a smart home. To the authors' knowledge, the floor tile is also the first design used to collect standing-BCG other than the weighing scale, which has been the only form used to collect standing-BCG for almost a decade since the re-emergence of BCG²⁵.

The next section details the design and evaluation of the tile, followed by the results of the evaluation study. We then discuss the practicality and efficacy of the tile before concluding the paper with key outcomes and recommendations for future work.

METHODS

This section provides an overview of the methods used to develop and evaluate the efficacy of the tile. The section starts with a discussion of the tile's design, followed by the experimental protocol used to collect data, and concludes with the validation of the tile's function.

Design of the instrumented floor tile

Platform design

The early prototype of the tile is shown in *Figure 1a*. Plexiglas was chosen as the platform material due to its non-conductive nature, easy availability, lightness, and sturdiness. The size of the prototype was selected to be 1 ft × 1 ft (30.5 cm × 30.5 cm) wide and 5/8 inches (1.6 cm) thick as it mimicked the size of a floor tile that was large enough for a person's feet to fit easily inside and thick enough to support their weight. Two types of sensors were installed: 4 load cells, each supporting up to 50 kg (EX204, Shenzhen Exact Sensor Instrument Co., Ltd, Shenzhen, China), on the bottom of the platform and four electrodes on the top of the platform (*Figure 1a*). Stainless steel was selected as the electrode material as it had good connectivity and was easy to keep clean. To minimize the bending moment on the platform, and thus maximize the weight that the tile can support without breaking, the load cells were placed directly beneath the electrodes where the user placed his or her feet. Four compartments and channels were made on the bottom of the platform by automatic milling machine according to *Figure 1 (b-f)*. For each compartment, 35 mm × 35 mm × 2.5 mm deep pocket was made so that the outer piece of load cell could fit snugly into the pocket and be flushed with the surface of the platform. In order for the load cell to function properly, the center piece must suspend in the air, so that the bending of the bridge connecting the center piece to the outer piece can be measured by the embedded strain gauge. As such, a smaller, deeper pocket (26 mm × 26 mm × 5 mm) was made at the center of the first pocket to have the center piece of load cell suspended in the air. The thickness of

the pocket (5 mm) was measured from the surface of the platform; the smaller pocket went 2.5 mm deeper from the wider pocket (*Figure 1*). The side view of the tile with a load cell is also shown in *Figure 1f*. With this configuration, the knob of the center piece projected out of the platform on which the load was applied. The placed load cells were secured with aluminum plates over the outer piece of each load cell. The electrodes were placed on top of the platform but the wire connection to each electrode went through the platform and guided out of the tile through 2.5 mm deep channels along with the wires of the load cells. The wire to each electrode was secured to the electrode using a nut and a bolt (i.e., tightening the electrode and the wire together) as soldering the wire on the stainless steel electrode was ineffective.

Ballistocardiogram circuit design

Signals from the load cells were processed to retrieve standing-BCG. *Figure 2a* shows the BCG conditioning circuit. In order to capture standing-BCG, four load cells were connected in Wheatstone bridge in a configuration adopted from a commercial weight scale (InnerScan BC-534 scale, Tanita, Tokyo, Japan). Each load cell was a half bridge with three terminals, as indicated by dotted boxes in *Figure 2a*. Since each load cell could handle a load of 50 kg, the tile had a total capacity to measure up to 200 kg. Load cells were connected to each other by connecting the end terminals. Two out of four middle terminals opposite to each other were connected to the power supply and the other two middle terminals were used as a signal output.

The sequence of the BCG conditioning circuit after the Wheatstone bridge was: a 2nd-order high-pass filter with cut-off frequency (f_c) 0.08 Hz, a differential amplifier with a gain (G) of 989, an AC coupling, a second order low-pass filter with a cut-off frequency (f_c) of 25 Hz, and finally a non-inverting amplifier with a gain of 100 dB (*Figure 2a*). The total gain of the circuit was approximately 100 dB. The passive high-pass filter prior to the first stage differential amplifier was used to suppress DC offset (i.e., common mode) from the Wheatstone bridge to minimize potential saturation at the output. The passive high-pass filter was selected from three different differential passive AC-coupling configurations were evaluated by Casas et al.²⁶; the configuration used produced the highest common-mode rejection ratio (CMRR) in near DC range (approximately 110 dB at 0.1 Hz). The same configuration was also used by Gonzalez-Landaeta et al. in their weight scale circuit²⁵. The remainder of the circuit was adopted from Inan et al.²⁷. In addition to Inan et al.'s design, we put a 1kΩ resistor (i.e., R₁₁ in *Figure 2a*) at the positive terminal

An instrumented floor tile

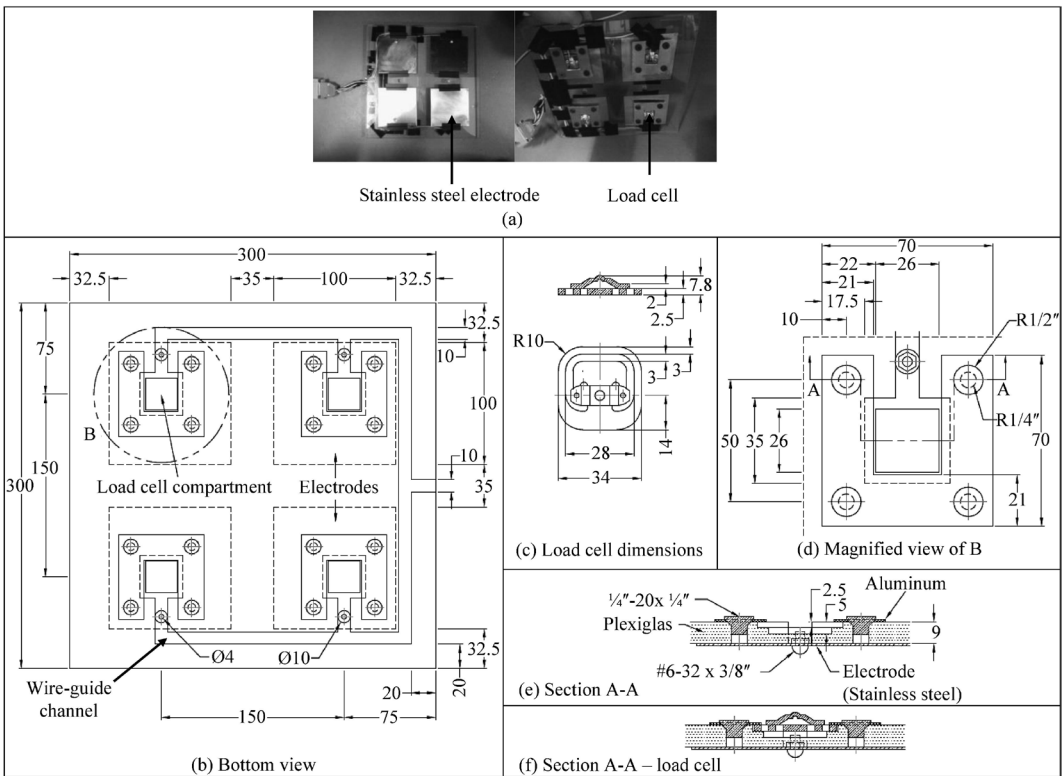


Figure 1. (a) Top (left) and bottom (right) view of the tile. Four electrodes were installed on the top and four load cells were installed in the load cell compartments on the bottom of the platform. The platform was made of Plexiglas. Wires were routed through the channels underneath the tile and exit to the side. (b) – (f) Computer aided diagram of the tile. All measurements are in millimeters if not indicated otherwise. (b) Bottom view of the tile. Each of the four load cell compartments, indicated with a circle B, contained a single load cell. The electrodes were on the opposite side or on the top of the platform, indicated by a dotted line (i.e., hidden line). (c) Dimensions of the load cell used. Each load cell has a capacity of 50kg. (d) Magnified view of the load cell compartment. The load cell was fixed by an aluminum plate covering the outer piece of the load cell and the aluminum plate was fixed by four flat-head screw bolts. (e) A cross-sectional view of the tile across the dash-dotted line (i.e., phantom line) A-A. The dash-dotted line goes through the middle of the flat-head screw bolts and then goes through the middle section of the compartment. (f) Cross-sectional view with the load cell installed in the compartment. The top piece of the load cell bears the weight.

of the non-inverting amplifier to balance the impedance to the negative terminal, thus reducing the bias current going into the operational-amplifier. Reduction in bias current in effect provided more voltage range for BCG swing or drift at the output caused by minor movements or body sway. Flow diagram of the BCG conditioning circuit is shown in Figure 2c and the collected signals are shown in Figure 3b.

All operational-amplifiers used for the BCG conditioning circuit generated ultra-low noise (i.e. 1 nV/ $\sqrt{\text{Hz}}$ at 1 kHz for AD8599 and 8 nV/ $\sqrt{\text{Hz}}$ at 1 kHz for AD8221 - both are intended for medical instrumentation applications) to support active noise filtering and to ensure noises generated by the operational-amplifiers were negligible in BCG conditioning. Signals from the tile were col-

lected using a National Instruments data acquisition board (DAQ with an NI cDAQ-9174 chassis and NI 9215 analog input module) and a LabVIEW 2011 interface. DAQ board was sampled with 128 Hz sampling frequency.

Foot Electrocardiogram circuit design

Sitting-F-ECG has significantly lower power compared to that of ECG measured from the chest (hereafter referred to as C-ECG). The range of linear operation of a typical ECG was $\pm 5 \text{ mV}$ and required a gain of about 1000 (i.e., 60 dB) if the location of the recording was close to the source of ECG (e.g., chest). As the power of the signal was significantly diminished as ECG reached the feet, the conditioning circuit with higher than 60 dB was required. As such, BCG conditioning circuit was adopted

An instrumented floor tile

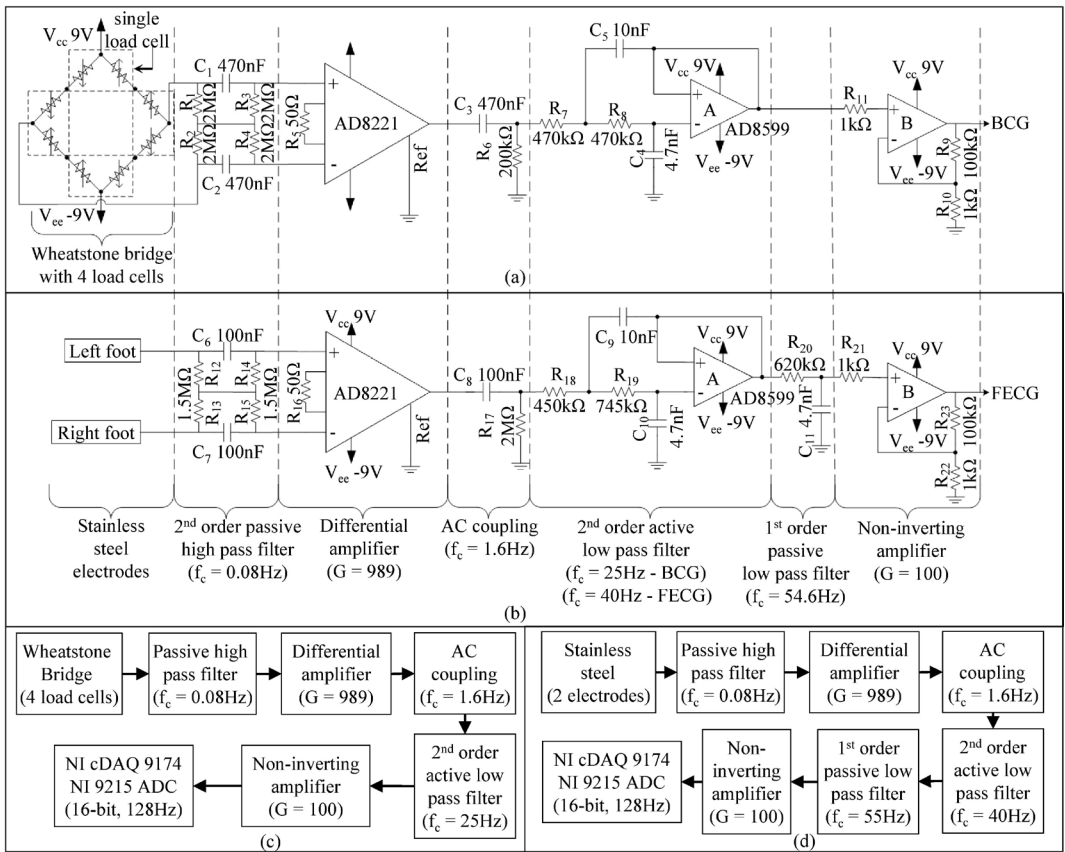


Figure 2. (a) BCG conditioning circuit. The signal from the Wheatstone bridge passed through an AC coupling, an instrumentation amplifier, another AC coupling, a 2nd order active low pass filter, and a non-inverting amplifier. The Wheatstone bridge was made using four half bridge load cells. Each load cell has three terminals and the end terminals were connected to the adjacent load cells and the middle terminal of each load cell was used either as an input or an output terminal. (b) F-ECG conditioning circuit. The differences of the circuit from that of BCG are that the cut-off frequency of active low pass filter has been set to 40 Hz and additional passive low pass filter has been added. (c) Flow diagram of BCG conditioning circuit. (d) Flow diagram of F-ECG conditioning circuit.

with minor modifications (Figure 2b). Two electrodes located at the foot hills were connected to the conditioning circuit. The electrodes at the foothills were used to maintain consistent contact with the skin as the weight of the body was supported by the hills while standing.

The difference between BCG and F-ECG conditioning circuits was that the cut-off frequency of 2nd-order active low-pass filter of F-ECG conditioning circuit had been increased from 25 Hz to 40 Hz. This was to incorporate a higher frequency component present in a typical ECG. As increasing the cut-off frequency allowed more powerline noise to pass through, additional first order passive low pass filter ($f_c = 55$ Hz) was used to suppress the noise. The rest of the functional specifications in the circuit remained the same as the BCG conditioning circuit. Flow diagram of the F-ECG conditioning circuit is shown in Figure 2d.

Data collection from the smart floor tile using healthy adults

After preliminary bench-top testing, the tile's efficacy was evaluated on healthy adults prior to testing on older adults (i.e., adults between 18 and 65 years of age who did not have implanted pacemakers, cardiovascular diseases, or respiratory diseases). Once the hardware and algorithms for healthy adults are reliable, the device can be tested on older adults from which algorithms for detecting abnormalities can be added to the system.

At the start of each trial, informed consent was obtained from each participant. Age, sex, weight, height, waist and hip circumference were obtained before attaching gold-standard (i.e., validated, commercially available) equipment to capture comparative signals. The gold-standard signal and device used to acquire the signal along with its locations on the body are indicated in Figure 3a, which is 3-lead C-ECG transmit-

An instrumented floor tile

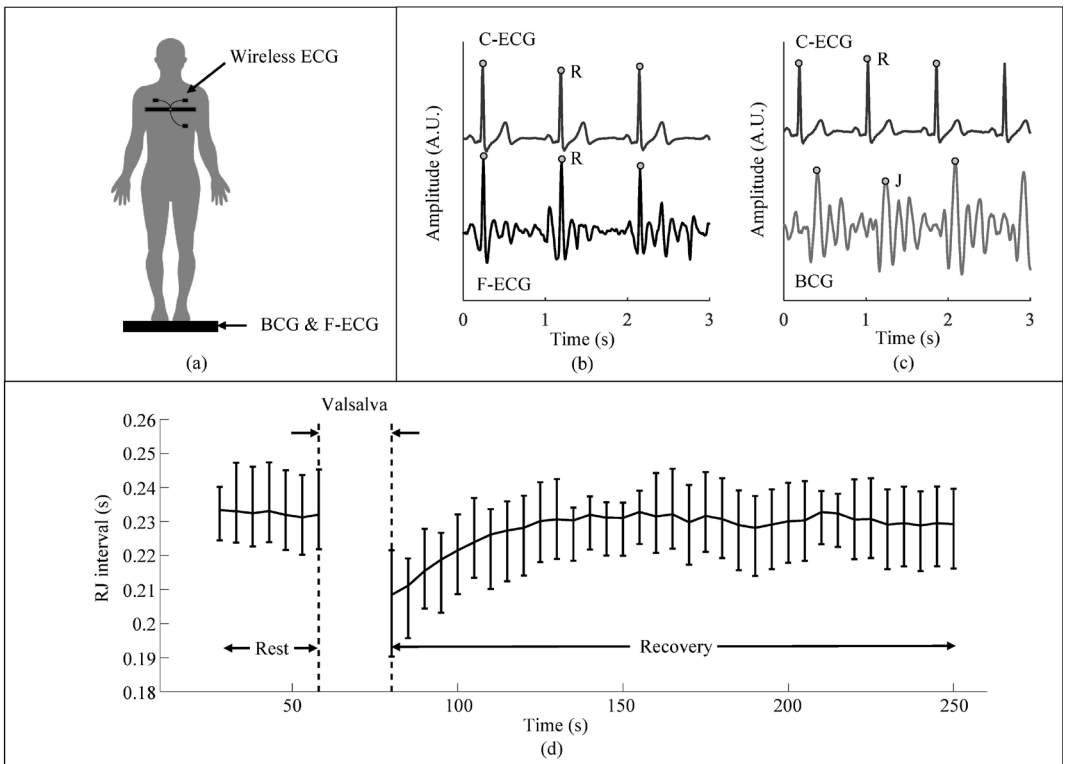


Figure 3. (a) Diagram of finished setup showing the placement of sensors on each subject during data collection. Gold-standard equipment included C-ECG, and the tile measured standing-BCG and sitting-F-ECG. All signals were recorded by one computer. (b) Collected gold-standard C-ECG, sitting-F-ECG signals collected from a subject in the data collection protocol during the seated scenario. (c) Collected C-ECG, standing-BCG signals during the standing scenario of the protocol. (d) Average RJ-interval for all participants aligned with respect to Valsalva maneuver. The error bars indicate first and third quartile of the RJ-interval data after the alignment. 5-second epoch was used to average the standing-BCG then RJ-interval was measured using the ensemble average of standing-BCG and C-ECG for each epoch. After the Valsalva maneuver, the reduced RJ-interval returned to the baseline.

ted wirelessly (Shimmer 2r ECG - Shimmer, Ireland) for continuous capture of HR. While other signals were measured, they were not included as they were irrelevant to work presented here. Each participant went through three different scenarios during the data collection protocol. However, only the first two scenarios, described below, were used in the evaluation of the tile:

(1) In the first scenario, each participant was asked to place their bare feet on the electrodes of the tile, relax their feet, and sit still in a chair for three minutes. The objective of this phase of the protocol was to check if the tile can be used for measuring sitting-F-ECG for a person sitting on a toilet in the bathroom. Three data sets were collected from each subject in this scenario. A 3-second portion of the collected signals from one subject in this scenario is shown in Figure 3b. (2) In the second scenario, each participant was asked to stand on the tile for 6 minutes. For the first minute, the participant was asked to stand without moving on the tile to obtain baseline parameters. At the one-minute mark, he or she was

asked to inhale, hold his or her breath, and apply pressure to the lungs without exhaling (known as the Valsalva maneuver) for 15 seconds to induce a change in BP 29. This was followed by 5 minutes of recovery while standing on the tile and breathing normally. Each participant was asked to repeat the protocol three times and hence three data sets were collected from each subject. A 3-second portion of the collected signals in this standing scenario is shown in Figure 3c.

The study protocol was approved by the Toronto Rehabilitation Institute's Research Ethics Board (REB12-038) and all trials were done at the HomeLab in Toronto Rehab Institute.

Foot Electrocardiogram and Ballistocardiogram signal analysis

The signals were filtered to remove residual signal drift and power-line noise using a band-pass finite-impulse response (FIR) filter with pass-band frequencies of 1-40 Hz (Hamming window). In order to validate the signals measured from the

tile, the following analysis involving R-peak detection, heart rate and RJ-interval were carried out from the data collected from 60 subjects.

Validation of sitting foot Electrocardiogram from the tile

To validate the sitting-F-ECG signal measured from the tile, the R-peaks in the sitting-F-ECG signal were compared to the corresponding R-peaks in the C-ECG signal. First, the Pan and Tompkins method was used to detect R-peaks in the C- and sitting-F-ECG signals. With each R-peak of C-ECG, R_i , as a center, where i denoted the peak index, a search for an R-peak was conducted in the sitting-F-ECG in the region $R_i \pm 16$ ms (2 samples). The purpose of using 16 ms window was to account for any possible time lag between the R-peak occurrences in the C- and sitting-F-ECG signals. If no R-peak was obtained in the sitting-F-ECG, an error counter 'Epsilon' was incremented while the presence of an R-peak in sitting-F-ECG incremented a correct counter denoted by 'Alpha'. Finally, the accuracy of the sitting-F-ECG signal was quantified as Alpha/N, where N was the total number of R-peaks in the C-ECG signal.

Heart rate estimation from the Ballistocardiogram

The highest peak in the BCG signal is called the J-peak. It is usually present within the first 300 ms portion of the BCG signal after the R-peak in the C-ECG^{15,29}. The time between consecutive J-peaks of the standing-BCG signal (i.e., JJ-interval) obtained from the tile was used to discern heart rate. The BCG J-peaks were found by searching for the highest peak in the standing-BCG within 0.3 s (300 ms) after the C-ECG peak, as this range was empirically determined to be large enough to capture the BCG J-peaks^{17,29}. C-ECG R-peaks were found via the simplified Pan and Tompkins method.

The tile's performance in measuring heart rate was evaluated by comparing the heart rate from standing-BCG to heart rate from C-ECG. Once the JJ-intervals were measured for each heartbeat of a participant, they were converted to a heart rate by taking the reciprocal and multiplying by 60. The standing-BCG heart rate was compared to the C-ECG heart rate and the error was calculated by dividing their difference by the heart rate

$$HR_{error} = \frac{HR_{C-ECG} - HR_{BCG}}{HR_{C-ECG}}, \quad (1)$$

where HR_{error} is the error in heart rate; $HR_{(C-ECG)}$ is C-ECG heart rate; and HR_{BCG} is BCG heart rate. Errors were calculated for all heartbeats from all participants and were used to find the mean error and standard deviation across the sample population. The data during the Valsalva maneuver was not used in the analysis.

Assessment of RJ-interval from the standing Ballistocardiogram

In addition to the heart rate, RJ-interval from the standing-BCG and C-ECG was calculated by estimating the time between R-peak of the C-ECG and corresponding J-peak, the highest peak of the standing-BCG. RJ-interval behavior after Valsalva maneuver was assessed in order to show that the ability of the tile to acquire standing-BCG properly. It was reported that the RJ-interval decreased post-Valsalva maneuver and returned to the baseline²⁹. The standing-BCG signal was segmented into individual traces which were averaged to reduce noise and assist in the robust detection of the J-peak. Again, the data during the Valsalva maneuver was removed as it was noisy due to movement artifacts.

Following this, the C-ECG and standing-BCG waveforms were separated into rest state and post-Valsalva state. Rest state was the period where the participant stood still for one minute prior to performing Valsalva maneuver. The two waveforms were divided into 5-second epochs. In each epoch, the C-ECG R-peaks R_i , where i again indicated the peak index, were detected using an automated Pan and Tompkins algorithm. The minimum RR-interval (RR_{min}) was estimated in each epoch and with R_i as fiducial points, $R_i + RR_{min}$ duration waveforms were extracted from the corresponding standing-BCG signal. The extracted standing-BCG waveforms in each epoch were averaged to obtain ensemble-averaged traces¹⁵ (hereafter referred to as the BCG heartbeats). The RJ-interval was estimated from these ensemble-averaged BCG heartbeats. The RJ-intervals estimated from all subjects in the study were aligned with respect to the Valsalva maneuver. Then, mean, first, and third quartiles were determined. The quartiles were used to indicate error range.

RESULTS

Sixty (60) participants (28 male, 32 female) were recruited with a mean age of 26.9 ± 6.1 years and mean body mass index (BMI) of 23.2 ± 3.4 kg/m². Data from three participants were excluded because they stopped the trial early; two of these participants had an abnormal blood pressure drop after the Valsalva maneuver and one participant had an abnormal ECG, namely pre-ventricular contractions. One participant showed involuntary movement during the data collection and was removed from the BCG analysis. Additionally, the BCG signals from five participants and the sitting-F-ECG signals from six participants were not recorded properly because of technical problems (i.e., poor connection and unavailability of gold-standard measurement). Thus, data from 51 participants were used for the BCG and F-ECG analysis. Note that BCG and F-ECG analysis have different sample populations; data from

four participants were used for BCG analysis only and data from four different participants (i.e., mutually exclusive to the four participants used for BCG analysis) were used for F-ECG analysis. Data from the remaining 47 participants were used for both BCG and F-ECG analyses.

Sitting foot Electrocardiogram signal analysis

To quantify the sitting-F-ECG measured from the tile, the number of correct R-peaks in the sitting-F-ECG was calculated and compared to the C-ECG in each trial for the sitting and standing protocols. It was observed that 89% of R-peaks in the C-ECG signal were also present in the sitting-F-ECG (across 54 subjects).

Standing Ballistocardiogram signal analysis

In terms of signal quality, standing-BCG showed high fidelity in capturing the heart rate when compared with the gold-standard, namely C-ECG. Based on the data from 51 participants (53,097 heartbeats), the heart rate based on standing-BCG had an average error rate (μ_{error}) of $1.8 \pm 4.3\%$ compared to the C-ECG gold-standard heart rate across all subjects. Standing-BCG was successfully acquired from all 54 participants in the standing scenario. In other words, we found that a clean standing-BCG signal could be acquired across a wide range of weight (47.2kg - 110.2kg) and BMI (17.4m²/kg - 30.9m²/kg).

RJ interval analysis

RJ-interval was reduced immediately after the Valsalva maneuver and returned to the baseline as shown in *Figure 3d*. This was in consonance with the existing studies on the BCG modality from modified weighing scale-based sensors. While the amplitude varied, the same pattern was observed after incorporating errors as shown in *Figure 3d*.

DISCUSSION

Heart rate based on BCG (JJ-interval) was compared with heart rate based on ECG (RR-interval). The results indicated that the measured standing-BCG from the tile was able to accurately estimate heart rate from a pool of 51 participants. Also, the trend in the RJ-interval measured after Valsalva maneuver showed a similar pattern as reported by existing studies^{15,29}. In terms of recovery of RJ-interval after Valsalva maneuver, although the degree of fluctuation of RJ-interval varied, the general trend showed that the tile successfully captured standing-BCG. The varying degree of RJ-interval fluctuation could be attributed to the unequal effort during Valsalva maneuver by each participant. While the time of Valsalva maneuver was kept consistent, some participants exerted less pressure to the chest, resulting in the damping effect of the maneuver. Despite this limitation, the

general trend showed that the tile could acquire RJ-interval, and thus standing-BCG.

Out of 153 repetitions (three repetitions per participant), 11 repetitions were removed. Trials that were removed from the analysis due to technical malfunction showed low signal-to-noise ratio (SNR). The technical malfunctions in collecting standing-BCG were mainly due to poor connections. Some of the erroneous repetitions caused by the lifting of feet from the electrodes, irregular movement artifacts and severe power-line noise due to technical malfunction were also excluded from the analysis. Electrodes were placed at the foot heels with the intention of having more secure contact to the skin because of weight-bearing though the heel during standing. This configuration however decreased the efficacy as foot heels were lifted slightly when sitting. Usage of electrodes at the sole region should be investigated in the future to address this issue. In terms of the design of the platform, the person standing on the tile had to put his or her bare feet together. As such, the size of the platform should be enlarged to accommodate different postures. In terms of additional improvement in structure, the tile thickness should mimic an actual tile and the durability of the tile should be tested to accommodate people with heavy weight (e.g., people with obesity). In one of the relevant studies, Linner et al. developed a smart wall that provides medical monitoring and assists activities of daily living (ADL). The performance of wall was evaluated in actual homes³⁰. The authors noted that refurbishment of the building was impractical in terms of cost and time. As such, making the system and its component modular (i.e., attachable, replaceable, and upgradable) was more effective³⁰. While the current prototype is still in its infant stage and is not ready for installment in an actual home, efforts should be made to build the tile system as a module that can simply be installed into the bathroom. Not only will this decrease the installment cost and time but also it will provide ways of easy maintenance, such as battery changes or connecting a power supply. Future work should also focus on ways to collect clean ECG with footwear such as socks by use of signal processing techniques and capacitive-coupled electrodes¹⁹.

While the BCG and F-ECG conditioning circuits were successful in retrieving the corresponding signals, it was observed that the circuits had a loading effect due to the relatively high output impedance of a stage compared to the input impedance of the next stage. This was caused by capacitors with low capacitance (i.e., C3 and C8 in *Figure 2*), and can be addressed by increasing the capacitance of the components or replacing the passive components with active components.

Due to the loading effect, the effective overall gains of the circuits may be smaller than what was determined originally (i.e., 100 dB). All wires from the sensors were routed through the bottom of the tile and a total of 16 wires (12 from load cells and four from the electrodes) were bundled through a small channel at a single exit point beneath the tile (*Figure 1b*). Through the course of these pilot trials, some of the wires inadvertently disconnected and had to be fixed later. Part of this design issue could be addressed by placing the Wheatstone bridge on the bottom of the tile instead of as part of the BCG conditioning circuit. By doing so, only four wires are needed for load cells and the number of wires exiting the tile would be halved. The conditioning circuits should eventually be miniaturized and embedded in the tile.

J-peaks of standing-BCG were detected using R-peaks of C-ECG as fiducial points. In the realistic scenario, C-ECG will not be available as a reference in detecting J-peaks of standing-BCG. Two possible solutions to this problem are to collect clean F-ECG while standing to use it to detect J-peaks and to use existing algorithms to detect J-peaks of standing-BCG without C-ECG. The former solution was tested but was found not viable since standing-F-ECG resulted in only 44% agreement with C-ECG due to noise from body sway and/or EMG as the muscles in the lower limbs were used to remain standing (*Figure 5b*)¹⁸. If the noise from the standing-F-ECG can be removed, it can then be used as a reference signal to detect J-peaks of standing-BCG. To implement the latter solution, existing algorithms for detecting peaks can be used. For example, Paalasmaa et al. and Bruser et al. developed algorithms to automatically detect heart rate based on transversal-BCG (e.g., supine position) via template-matching or machine learning techniques without ECG or other reference signals^{31,32}. These algorithms can be adopted to extract features of standing-BCG such as J-peak. Collecting clean standing-F-ECG is difficult to achieve at this point and is discussed further in the next section.

We examined how the tile functioned under the influence of movements such as hand washing and tooth brushing. The tile, however, was not robust enough to collect standing-BCG while the person standing on the tile was doing an activity due to motion artifacts; the participants had to stand still in order to collect a usable standing-BCG. It must be noted however that movement artifact is an open issue when working with standing-BCG and should be treated as a different research problem (i.e., the problem of movement artifact is out of the scope of this work). While there are some previous researches that used extra sensors and signal processing to reduce a small amount of vibration noise or flag

the section of standing-BCG that is corrupted by movement artifact³³, to the best of our knowledge, there is currently no viable method to remove movement artifact completely from standing-BCG. With respect to the older adult population, this limitation poses a significant challenge as there may be older adults who do not have physical ability to stand still (e.g., the presence of tremor or frailty). Hence, a possible solution is to further investigate noise reduction and motion artifact removal algorithms to improve the quality of the measured BCG signal. A more robust solution will be the development of a prompting system as part of the tile system to help the older adult being monitored to stand still for a few seconds so that a proper standing-BCG is recorded. Czarnuch et. al proposed a similar prompting system that uses audio and video prompts to aid older adults with dementia to wash their hands³⁴.

In the next iteration of the system, a software platform should be created that conveys data to users, such as delivering and displaying appropriately formatted data to various relevant stakeholders. There are several models that can be adopted from the literature^{30,35}. As the aim of the unobtrusive monitoring is early detection of possible adverse events, the platform should have an ability to monitor the short-term and long-term trends of one's health and detect any unusual deviations. The platform should also have intuitive operation system and incorporate features like speech or gesture-based commands as well as an intuitive feedback system.

Overall readiness of the current technology is still at an early prototype stage, requiring further development and validation before it can be implemented in a real-world environment. Insights from medicine, electronics, signal processing, architecture/structural engineering, and user interface development must be incorporated in the next stages of the project. Once the device is ready in all of these areas, it can then go through field testing to validate the monitoring of the health of older adults.

These results suggest that the tile is capable of measuring heart rate close to the medical equipment used in the hospital without attaching any wires to the body when the person is standing or sitting still with bare feet. If two tiles were installed in the bathroom - one in front of the sink and one in front of the toilet (*Figure 4*) - heart rate could be captured whenever the person performed bathroom routines. The location and low-profile of the tile would support compliance, eliminate the need for the user to actively engage with the technology, and would help avoid the stigma (e.g., feeling embarrassed or uncomfortable) by having medical monitoring equipment at home. The captured heart rate of the person can be sent to a central

An instrumented floor tile

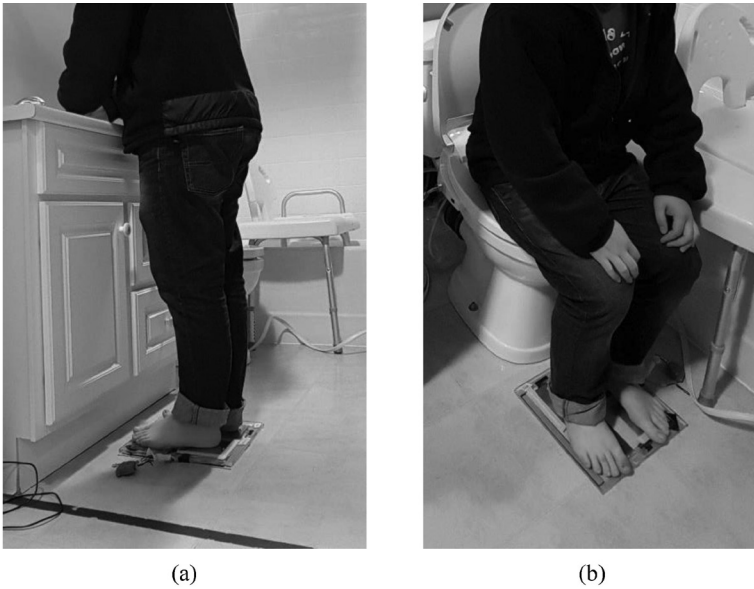


Figure 4. Example usage of the tile (a) Standing in front of the bathroom sink. (b) Sitting on the toilet.

computer at home, which can forward the information to relevant stakeholders (e.g., care givers, clinicians, and/or the person being monitored).

Collection of sitting Ballistocardiogram

As mentioned above, it is currently not feasible to collect clean standing-BCG when there are movement artifacts. A possible alternative to this is to use a different form factor. The smart floor tile was intended to be used for both sitting and standing. As such, taking advantage of the sitting form factor to collect BCG may address the limitation of movement artifacts that are present while standing. BCG while sitting (sitting-BCG) was collected during the trial in order to assess the feasibility. The result of the analysis is presented here as a peripheral work.

The signal measured during the sitting protocol via BCG conditioning circuit was extremely noisy and hence no heart rate could be estimated from the raw data. The signal was examined by applying the 5-second epoch ensemble averaging method to the signal which resulted in periodic BCG-like heartbeats with high SNR. Note the word “BCG-like heartbeats” here as it is uncertain that the signal collected is indeed BCG based on the data we have. In typical BCG measured during sitting, much of the force composing BCG has been transferred to the seat; the person’s weight is mainly transferred to the chair rather than their feet, therefore the contact force on the floor tile is much less than the standing condition. Based on this reasoning, there are two possible ways of interpreting the recorded signal. Firstly, it is possible that the signal is a much weaker version of BCG measured from the seat of a chair¹⁹. Another possibility is that the BCG-like signal recorded is actually a local pulse (i.e., change in volume/pressure in blood vessels of particular body part such as the feet due to the beating of the heart) rather than BCG (i.e., reactive force to the heartbeat appearing as slight oscillation of the body weight). Figure 5a shows a 5-second ensemble-averaged heartbeat during the standing and sitting scenario from one subject. While some of the morphology of the BCG-like signal from sit-

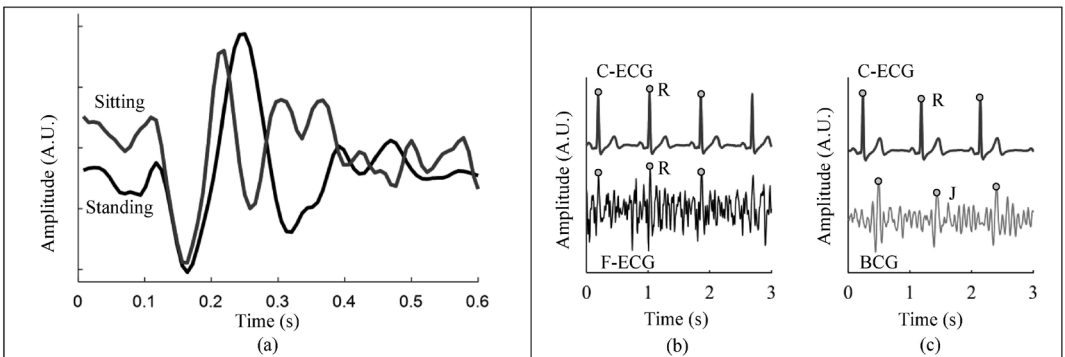


Figure 5. (a) Ensemble-averaged BCG heartbeats (5-second epoch) during sitting and standing phase of the data protocol from one subject. (b) Collected gold-standard C-ECC, standing-F-ECC signals collected from a subject in the data collection protocol during the standing scenario. Standing-F-ECC is corrupted by EMG and body sway (c) Collected C-ECC, sitting-BCG signals during the seated scenario of the protocol. Sitting-BCG is significantly weaker compared to standing-BCG as BCG force may have been dampened by the chair seat.

ting differed from that of standing-BCG, a similar effect had been observed in seated body vibrations in prior literature^{15,36}. The change in morphology appeared in the form of an additional peak next to the J-peak in the sitting-BCG heartbeat (*Figure 5a*). To the best of our knowledge, acquisition of BCG-like signal from the feet during sitting has not been investigated before and this is the first example of such technique. As such, while the morphology and the timing of the signal is similar to BCG, we add a note of caution that further investigation needs to be made to validate what was measured is actual BCG. Namely, sitting-BCG from the tile, local pulse from the feet (e.g., photoplethysmogram), sitting-BCG from a chair, and C-ECG should be collected simultaneously to verify that the sitting-BCG from the tile corresponds to the sitting-BCG from the chair and differs from the local pulse from the feet. Sitting-BCG is shown in *Figure 5b*.

Based on the observations above, it is difficult to determine if clean and usable sitting-BCG can be collected. Thus, further investigation is required to ascertain if the acquisition of the signal is feasible with the implementation of more advanced hardware and signal processing.

CONCLUSION

The goal of the work presented above was to create an unobtrusive, zero-effort device that can be used to measure BCG and ECG to support cardiovascular health monitoring for older adults living at home. Based on this goal, we developed a prototype of a floor tile that can be incorporated in the user's environment more naturally as compared to existing devices. In addition to the standing-BCG acquisition, the tile uses sensors to unobtrusively detect ECG without the need to attach electrodes to the body. Our evaluation with 54 healthy participants showed that the parameters from the standing-BCG measured by the tile agreed with the literature and sitting-FECG agreed with conventional ECG with 89% accuracy. While the smart tile needs further investigation and improvement, it shows promising potential as a novel way of collecting standing-BCG and sitting-F-ECG without any effort on the part of the person being monitored. As such, this work constitutes a step forward in the creation of a smart home capable of supporting older adults' health.

References

1. The Chief Public Health Officer's Report on the State of Public Health in Canada, 2014: Public Health in the Future -Changing Demographics, Aging and Health [Internet]; c2014 [cited 2015 05/25]. <http://www.phac-aspc.gc.ca/cphorsphc-respcac-sp/2014/chang-eng.php>; retrieved May 28, 2018
2. Mozaffarian D, Benjamin EJ, Go AS, Arnett DK, Blaha MJ, Cushman M, Das SR, de Ferranti S, Després JP, Fullerton HJ, Howard VJ, Huffman MD, Isasi CR, Jiménez MC, Judd SE, Kissela BM, Lichtman JH, Lisabeth LD, Liu S, Mackey RH, Magid DJ, McGuire DK, Mohler ER, Moy CS, Muntner P, Mussolino ME, Nasir K, Neumar RW, Nichol G, Palaniappan L, Pandey DK, Reeves MJ, Rodriguez CJ, Rosamond W, Sorlie PD, Stein J, Towfighi A, Turan TN, Virani SS, Woo D, Yeh RW, Turner MB, and on behalf of the American Heart Association Statistics Committee and Stroke Statistics Subcommittee. Executive summary: Heart disease and stroke statistics--2016 update: A report from the american heart association. *Circulation* 2016 Jan 26;133(4):447-454; <https://doi.org/10.1161/CIR.0000000000000366>
3. Benjamin EJ, Blaha MJ, Chiuve SE, Cushman M, Das SR, Deo R, de Ferranti SD, Floyd J, Fornage M, Gillespie C, Isasi CR, Jiménez MC, Jordan LC, Judd SE, Lackland D, Lichtman JH, Lisabeth L, Liu S, Longenecker CT, Mackey RH, Matsushita K, Mozaffarian D, Mussolino ME, Nasir K, Neumar RW, Palaniappan L, Pandey DK, Thiagarajan RR, Reeves MJ, Ritchey M, Rodriguez CJ, Roth GA, Rosamond WD, Sasson C, Towfighi A, Tsao CW, Turner MB, Virani SS, Voeks JH, Willey JZ, Wilkins JT, Wu JHY, Alger HM, Wong SS, Muntner P, and on behalf of the American Heart Association Statistics Committee and Stroke Statistics Subcommittee. Heart disease and stroke statistics-2017 update: A report from the american heart association. *Circulation* 2017 Mar 7;135(10):e146-603. <https://doi.org/10.1161/CIR.0000000000000485>
4. Bradley EH, Curry L, Horwitz LI, Sipsma H, Wang Y, Walsh MN, Goldmann D, White N, Pina IL, Krumholz HM. Hospital strategies associated with 30-day readmission rates for patients with heart failure. *Circ Cardiovasc Qual Outcomes* 2013 Jul;6(4):444-450. <https://doi.org/10.1161/CIR-COUTCOMES.111.000101>
5. Koehler F, Winkler S, Schieber M, Sechtem U, Stangl K, Böhm M, Boll H, Baumann G, Honold M, Koehler K, Gelbrich G, Kirwan BA, Anker SD. Impact of remote telemedical management on mortality and hospitalizations in ambulatory patients with chronic heart failure: The telemedical interventional monitoring in heart failure study. *Circulation* 2011 May 3;123(17):1873-1880. <https://doi.org/10.1161/CIRCULATIONAHA.111.018473>
6. Chaudhry SI, Matterna JA, Curtis JP, Spertus JA, Herrin J, Lin Z, Phillips CO, Hodshon BV, Cooper LS, Krumholz HM. Telemonitoring in patients with heart failure. *N Engl J Med* 2010 Dec 9;363(24):2301-2309. <https://doi.org/10.1056/NEJMoa1010029>
7. Wade MJ, Desai AS, Spettell CM, Snyder AD, McGowan-Stackewicz V, Kummer PJ, Maccoby MC, Krakauer RS. Telemonitoring with case management for seniors with heart failure. *Am J Manag Care* 2011 Mar 1;17(3):e71-79. [47949 pii]
8. Goldberg LR, Piette JD, Walsh MN, Frank TA, Jaski

- BE, Smith AL, Rodriguez R, Mancini DM, Hopton LA, Orav EJ, Loh E. Randomized trial of a daily electronic home monitoring system in patients with advanced heart failure: The weight monitoring in heart failure (WHARF) trial. *Am Heart J* 2003 Oct;146(4):705-712. [https://doi.org/10.1016/S0002-8703\(03\)00393-4](https://doi.org/10.1016/S0002-8703(03)00393-4)
9. Cleland JG, Louis AA, Rigby AS, Janssens U, Balk AH, TEN-HMS Investigators. Noninvasive home telemonitoring for patients with heart failure at high risk of recurrent admission and death: The trans-european network-home-care management system (TEN-HMS) study. *J Am Coll Cardiol* 2005 May 17;45(10):1654-1664. [S0735-1097(05)00484-5]
 10. Alzheimer's Association. 2017 alzheimer's disease facts and figures. Washington, D.C.: Alzheimer's Association; 2017
 11. Liu L, Stroulia E, Nikolaidis I, Miguel-Cruz A, Rios Rincon A. Smart homes and home health monitoring technologies for older adults: A systematic review. *Int J Med Inform* 2016 Jul;91:44-59. <https://doi.org/10.1016/j.ijmedinf.2016.04.007>
 12. Muse ED, Barrett PM, Steinhubl SR, Topol EJ. Towards a smart medical home. *The Lancet* 2017 28 January-3 February 2017;389(10067):358. <http://www.sciencedirect.com/science/article/pii/S014067361730154X?via%3Dihub>; retrieved May 28, 2018
 13. Mihailidis A, Boger J, Hoey J, Jiancaro T. Zero effort technologies: Considerations, challenges, and use in health, wellness, and rehabilitation. *Synthesis Lectures on Assistive, Rehabilitative, and Health-Preserving Technologies* 2011;1(2):1-94.
 14. Kim CS, Ober SL, McMurtry MS, Finegan BA, Inan OT, Mukkamala R, Hahn JO. Ballistocardiogram: Mechanism and potential for nonobtrusive cardiovascular health monitoring. *Sci Rep* 2016 Aug 9;6:31297. <https://doi.org/10.1038/srep31297>
 15. Javaid AQ, Wiens AD, Fesmire NF, Weitnauer MA, Inan OT. Quantifying and reducing posture-dependent distortion in ballistocardiogram measurements. *IEEE J Biomed Health Inform* 2015 Sep;19(5):1549-1556. <https://doi.org/10.1109/BHI.2016.7455956>
 16. Inan OT, Migeotte PF, Park KS, Etemadi M, Tavakolian K, Casanella R, Zanetti J, Tank J, Funtova I, Prisk GK, Di Rienzo M. Ballistocardiography and seismocardiography: A review of recent advances. *IEEE J Biomed Health Inform* 2015 Jul;19(4):1414-1427. <https://doi.org/10.1109/JBHI.2014.2361732>
 17. Javaid AQ, Ashouri H, Tridandapani S, Inan OT. Elucidating the hemodynamic origin of ballistocardiographic forces: Toward improved monitoring of cardiovascular health at home. *IEEE J Transl Eng Health Med* 2016 Mar 24;4:1900208. <https://doi.org/10.1109/JBHI.2015.2441876>
 18. Shin JH, Lee KM, Park KS. Non-constrained monitoring of systolic blood pressure on a weighing scale. *Physiol Meas* 2009 Jul;30(7):679-93. <https://doi.org/10.1088/0967-3334/30/7/011>
 19. Baek HJ, Chung GS, Kim KK, Park KS. A smart health monitoring chair for noninvasive measurement of biological signals. *IEEE Trans Inf Technol Biomed* 2012 Jan;16(1):150-158. <https://doi.org/10.1109/TITB.2011.2175742>
 20. Paalasmaa J, Waris M, Toivonen H, Leppakorpi L, Partinen M. Nonobtrusive online monitoring of sleep at home. *Conf Proc IEEE Eng Med Biol Soc* 2012;2012:3784-88. <https://doi.org/10.1109/EMBC.2012.6346791>
 21. Bruser C, Diesel J, Zink MDH, Winter S, Schauer P, Leonhardt S. Automatic detection of atrial fibrillation in cardiac vibration signals. *Biomedical and Health Informatics, IEEE Journal of* 2013;17(1):162-171. <https://doi.org/10.1109/TITB.2012.2225067>
 22. Etemadi M, Inan OT, Heller JA, Hersek S, Klein L, Roy S. A wearable patch to enable long-term monitoring of environmental, activity and hemodynamics variables. *IEEE Trans Biomed Circuits Syst* 2016 Apr;10(2):280-288. <https://doi.org/10.1109/TBCAS.2015.2405480>
 23. He DD, Winokur ES, Sodini CG. An ear-worn continuous ballistocardiogram (BCG) sensor for cardiovascular monitoring. *Conf Proc IEEE Eng Med Biol Soc* 2012;2012:5030-5033. <https://doi.org/10.1109/EMBC.2012.6347123>
 24. Withings. The science behind body cardio and pulse wave velocity: Heart health and body composition wi-fi scale. 2016. http://media.dcrainmaker.com/images/2016/06/Withings-Science_behind_PWV.pdf; retrieved May 28, 2018
 25. Gonzalez-Landaeta R, Casas O, Pallas-Areny R. Heart rate detection from an electronic weighing scale. *Physiol Meas* 2008 Aug;29(8):979-988. <https://doi.org/10.1088/0967-3334/29/8/009>
 26. Casas O, Spinelli EM, Pallas-Areny R. Fully differential AC-coupling networks: A comparative study. *IEEE Transactions on Instrumentation and Measurement* 2009 January;58(1):94-98. <http://ieeexplore.ieee.org/stamp/stamp.jsp?arnumber=4568419>; retrieved May 28, 2018
 27. Inan OT, Etemadi M, Paloma A, Giovangrandi L, Kovacs GT. Non-invasive cardiac output trending during exercise recovery on a bathroom-scale-based ballistocardiograph. *Physiol Meas* 2009 Mar;30(3):261-274. <https://doi.org/10.1088/0967-3334/30/3/003>
 28. Webster J. *Medical instrumentation: Application and design*. 4th Ed ed. John Wiley & Sons; 2011
 29. Etemadi M, Inan OT, Giovangrandi L, Kovacs GT. Rapid assessment of cardiac contractility on a home bathroom scale. *IEEE Trans Inf Technol Biomed* 2011 Nov;15(6):864-869. <https://doi.org/10.1109/TITB.2011.2161998>
 30. Linner T, Güttler J, Bock T, Georgoulas C. Assistive robotic micro-rooms for independent living. *Automation in Construction* 2015 March 2015;51:8-22. <http://dx.doi.org/10.1016/j.autcon.2014.12.013>
 31. Paalasmaa J, Toivonen H, Partinen M. Adaptive heartbeat modelling for beat-to-beat heart rate measurement in ballistocardiograms. *IEEE J Biomed Health Inform* 2014 Mar 28. <https://doi.org/10.1109/JBHI.2014.2314144>
 32. Bruser C, Winter S, Leonhardt S. Robust inter-beat interval estimation in cardiac vibration signals. *Physiol Meas* 2013 Feb;34(2):123-138. <https://doi.org/10.1088/0967-3334/34/2/123>
 33. Inan OT, Kovacs GT, Giovangrandi L. Evaluating

- the lower-body electromyogram signal acquired from the feet as a noise reference for standing ballistocardiogram measurements. *IEEE Trans Inf Technol Biomed* 2010 Sep;14(5):1188-1196. <https://doi.org/10.1109/TITB.2010.2044185>
34. Czarnuch S, Cohen S, Parameswaran V, Mihailidis A. A real-world deployment of the COACH prompting system. *J Ambient Intell Smart Environ*. 2013 sep;5(5):463-478. <http://dl.acm.org/citation.cfm?id=2594708.2594713>; retrieved May 28, 2018
35. Rantz MJ, Skubic M, Miller SJ, Galambos C, Alexander G, Keller J, Popescu M. Sensor technology to support aging in place. *J Am Med Dir Assoc* 2013 Jun;14(6):386-391. <https://doi.org/10.1016/j.jamda.2013.02.018>
36. Kitazaki S, Griffin MJ. Resonance behaviour of the seated human body and effects of posture. *J Biomech* 1998 Feb;31(2):143-149. [S0021929097001267]
-